

# Charge Transport and Rectification in Arrays of SAM-Based Tunneling Junctions

Christian A. Nijhuis, William F. Reus, Jabulani R. Barber, Michael D. Dickey, and George M. Whitesides\*

Department of Chemistry and Chemical Biology, Harvard University, 12 Oxford Street, Cambridge, Massachusetts 02138

**ABSTRACT** This paper describes a method of fabrication that generates small arrays of tunneling junctions based on self-assembled monolayers (SAMs); these junctions have liquid-metal top-electrodes stabilized in microchannels and ultraflat (template-stripped) bottom-electrodes. The yield of junctions generated using this method is high (70–90 %). The junctions examined incorporated SAMs of alkanethiolates having ferrocene termini (11-(ferrocenyl)-1-undecanethiol, SC<sub>11</sub>Fc); these junctions rectify currents with large rectification ratios ( $R$ ), the majority of which fall within the range of 90–180. These values are larger than expected (theory predicts  $R \leq 20$ ) and are larger than previous experimental measurements. SAMs of  $n$ -alkanethiolates without the Fc groups (SC <sub>$n$ -1</sub>CH<sub>3</sub>, with  $n = 12, 14, 16, \text{ or } 18$ ) do not rectify ( $R$  ranged from 1.0 to 5.0). These arrays enable the measurement of the electrical characteristics of the junctions as a function of chemical structure, voltage, and temperature over the range of 110–293 K, with statistically large numbers of data ( $N = 300\text{--}800$ ). The mechanism of rectification with Fc-terminated SAMs seems to be charge transport processes that change with the polarity of bias: from tunneling (at one bias) to hopping combined with tunneling (at the opposite bias).

**KEYWORDS** Nanoelectronics, molecular electronics, charge transport, self-assembled monolayers, rectification, charge transfer

Molecular electronics<sup>1</sup> originally promised that molecule(s) bridging two or more electrodes would generate electronic function and overcome the scaling limits of conventional semiconductor technology.<sup>2–4</sup> Although, so far, there have been no commercially successful molecular electronic devices, the subject of charge transport in molecularly scaled systems is unquestionably *fundamentally* interesting.

Much of the work on the physical and physical–organic mechanisms of charge-transport has used self-assembled monolayers (SAMs) of alkanethiolates on Au and Ag substrates, with these metals as the bottom-electrode, but a variety of top-electrodes. We also use SAMs of organic thiolates on Ag in our studies. Fabricating even simple molecular circuits using SAMs of alkanethiolates chemisorbed on Au or Ag substrates and contacted by metal top-electrodes has been a challenge: most fabrication techniques produce junctions in low yields.<sup>5</sup> These junctions have been dominated by artifacts<sup>6</sup> (especially conducting filaments<sup>7–10</sup>) and generate too few reliable data for statistical analysis (the work of Lee et al. provides an exception<sup>11</sup>). Physical–organic studies connecting molecular structure and electrical properties have been difficult or impossible to carry out with most junctions based on SAMs of Au or Ag, and studies that include measurements as a function of temperature—measurements necessary to determine the mechanism(s) of charge transport across SAM-based junctions—have also

been difficult (the work of Allara et al.<sup>12</sup> and Tao et al.<sup>13</sup> provide examples of successful studies).

An alternative approach to studies of charge transport through organic monolayers is that of Kahn et al., Cahen et al., and Boecking, who covalently attach monolayers of alkyl chains to a doped Si substrate via hydrosilylation of alkenes with a H-passivated Si surface,<sup>14</sup> and contact these monolayers using a Hg top-electrode.<sup>15</sup> These Si-alkyl//Hg junctions are unquestionably useful for studying charge transport and are more stable than have been most junctions in which SAMs of alkanethiolates chemisorbed on Au or Ag are directly contacted by a metal top-electrode, but like other techniques, Si-alkyl//Hg junctions have both advantages and disadvantages. The primary advantage is that contacting the monolayer with a Hg drop does not damage the monolayer (by penetration through pinholes or diffusion of mercury vapor through the SAM). As a result, measurements using these junctions appear to be quite reproducible across the set of junctions reported (although the interpretation of these measurements would benefit from more information concerning the statistical distribution of data, and yields of reported junctions, compared to unreported junctions or shorts). Another advantage of these junctions is that they support measurements of charge transport over a limited range of temperatures<sup>16</sup> ( $T = 250\text{--}330$  K), measurements which have yielded valuable information on the mechanism of charge transport in these junctions. Among the disadvantages of organic monolayers covalently bound to Si is that they are less well ordered than SAMs of alkanethiolates on Au or Ag, and it is difficult synthetically to achieve large variations in the structure of the organic R group. With respect to charge transport, these junctions are mechanistic-

\* To whom correspondence should be addressed, gwhitesides@gmwhgroup.harvard.edu.

Received for review: 05/31/2010

Published on Web: 08/18/2010



cally complex, in that they incorporate not just a tunneling barrier but a Schottky barrier as well.<sup>17</sup>

We describe a technique that exploits the advantages of SAMs of alkanethiolates chemisorbed on Ag while overcoming many of the challenges faced in previous studies of SAM-based junctions. Our technique generates small arrays (seven junctions) of SAM-based junctions with satisfactory yields (70–90%) of working devices; this technique makes it possible to conduct physical–organic studies with statistically large numbers of data ( $N = 300–800$ ) and to do so over a range of temperatures ( $T$ ) sufficiently broad (110–293 K) to provide useful information about the mechanisms of charge transport.

We investigated two systems. (i) Junctions based on SAMs of  $n$ -alkanethiolates ( $SC_{n-1}CH_3$ , with  $n = 12, 14, 16,$  or  $18$ ); these junctions show, as expected,<sup>6</sup> tunneling as the dominant mechanism of charge transport. (ii) Junctions based on SAMs of alkanethiolates terminated with ferrocene (1-(ferrocenyl)-1-undecanethiol,  $SC_{11}Fc$ ) groups; these junctions rectify currents, and thus act as molecular diodes with rectification ratios  $R \approx 1.3 \times 10^2$  (eq 1). In eq 1,  $J =$  current density ( $A/cm^2$ ) and  $V =$  voltage (V).

$$R \equiv |J(-1.0 \text{ V})|/|J(+1.0 \text{ V})| \quad (1)$$

Studying the rectification ratios, rather than current densities, has the advantage that the current measured in one direction of bias serves as a reference for the current measured at the opposite bias and, thus, eliminates many of the uncertainties related to contact areas or contact resistances. Some uncertainties may, however, still be present. For instance, structurally different molecular dipoles might, in principle, exist at the interfaces between the molecules and the two electrodes; this difference could affect  $R$  by causing  $J$  to depend on the polarity of applied bias. We believe, however, that such factors do not contribute significantly to rectification. Junctions containing  $n$ -alkanethiols essentially do not rectify ( $R < 5$ ), and these SAMs make interfaces with the two electrodes that are, we believe, likely to be representative of most alkanethiolate SAM-based junctions. As a result, we infer that a junction at one bias is a good reference for the same junction at the opposite bias.

Most research, both theoretical and experimental, that has had the objective of developing the molecular analogue of a diode has been based on the so-called “electron donor–bridge–acceptor” compounds described in a seminal paper by Aviram and Ratner.<sup>18</sup> Tunneling junctions incorporating these molecules,<sup>19–21</sup> and others<sup>22,23</sup> (including one example reported by us<sup>24</sup>), have rectified currents, but neither the mechanism of charge transport nor the origin of the observed rectification have been unambiguously established in any junction. Four factors underlie this ambiguity: (i) structural information on SAMs only exists for a relatively small number of molecular precursors;<sup>25</sup> virtually

no structural information is available for SAMs incorporating molecules with the donor–bridge–acceptor architecture, due to their structural complexity. (ii) Asymmetries other than an electric dipole, present either in the SAMs themselves or in the junctions, can contribute to rectification;<sup>26</sup> many of the previous studies do not rule out these other possible sources of rectification using appropriate controls and statistics. (iii) The reported rectification ratios have typically been low ( $1 < R < 5$ <sup>22–24</sup>). Without adequate statistical support, most of these values are not distinguishable from  $R \sim 1$ . (iv) Measurements of  $J–V$  as a function of temperature—measurements necessary to determine the mechanisms of charge transport—have not been conducted.<sup>12,13,27</sup>

These studies, as a group, have not considered molecular rectifiers in which a change occurs in the mechanism of charge transport (e.g., from tunneling to hopping) as applied bias switches polarity; below we show that such junctions have the potential to yield large rectification ratios ( $R > 10^3$ ).

We have reported that an eutectic alloy of gallium and indium (EGaIn), with its superficial layer of  $Ga_2O_3$ , can be molded into cone-shaped tips that are useful to form electrical contacts with SAMs;<sup>28,29</sup> the properties of  $Ga_2O_3/EGaIn$  resemble that of a non-Newtonian fluid.<sup>30</sup> This method affords SAM-based junctions with high yields of working devices and enables statistical analysis through the collection of large amounts of data. These junctions—with the top-electrode suspended from a syringe—are convenient to use, but they lack the encapsulation and addressability needed to operate in a pressure- and temperature-controlled chamber.

Here we report a method (Figure 1, see Supporting Information), based on  $Ga_2O_3/EGaIn$  stabilized in microchannels in a transparent polymer (PDMS), that we used to construct arrays of SAM-based tunneling junctions that (i) are mechanically stable, (ii) do not suffer from alloying between metal electrodes, (iii) do not require metal deposition either by electron-beam evaporation or by sputtering directly onto SAMs, (iv) do not require intermediate layers of conducting polymers, or rigorous/empirical processing steps, and (v) make it possible to perform  $J–V$  measurements as a function of temperature over a broad range of temperatures (110–293 K). Figure 2 shows optical micrographs of a complete device.

Panels F and G of Figure 1 show idealized views of the junctions. In reality, the SAMs have defects due to (i) step edges, (ii) phase boundaries, (iii) pin holes, (iv) impurities, and (v) grain boundaries.<sup>25</sup> To reduce the number of defects in the SAM relative to the number present in the rough top-surface of evaporated silver, we used ultraflat, template-stripped silver ( $Ag^{TS}$ ) electrodes embedded in cured optical adhesive (OA).<sup>31</sup> It is important to embed the electrodes in OA to prevent free-standing structures of Ag on the wafer, with edges at which the SAMs cannot pack densely,<sup>32</sup> that may cause shorts once the channels are filled with  $Ga_2O_3/EGaIn$ .

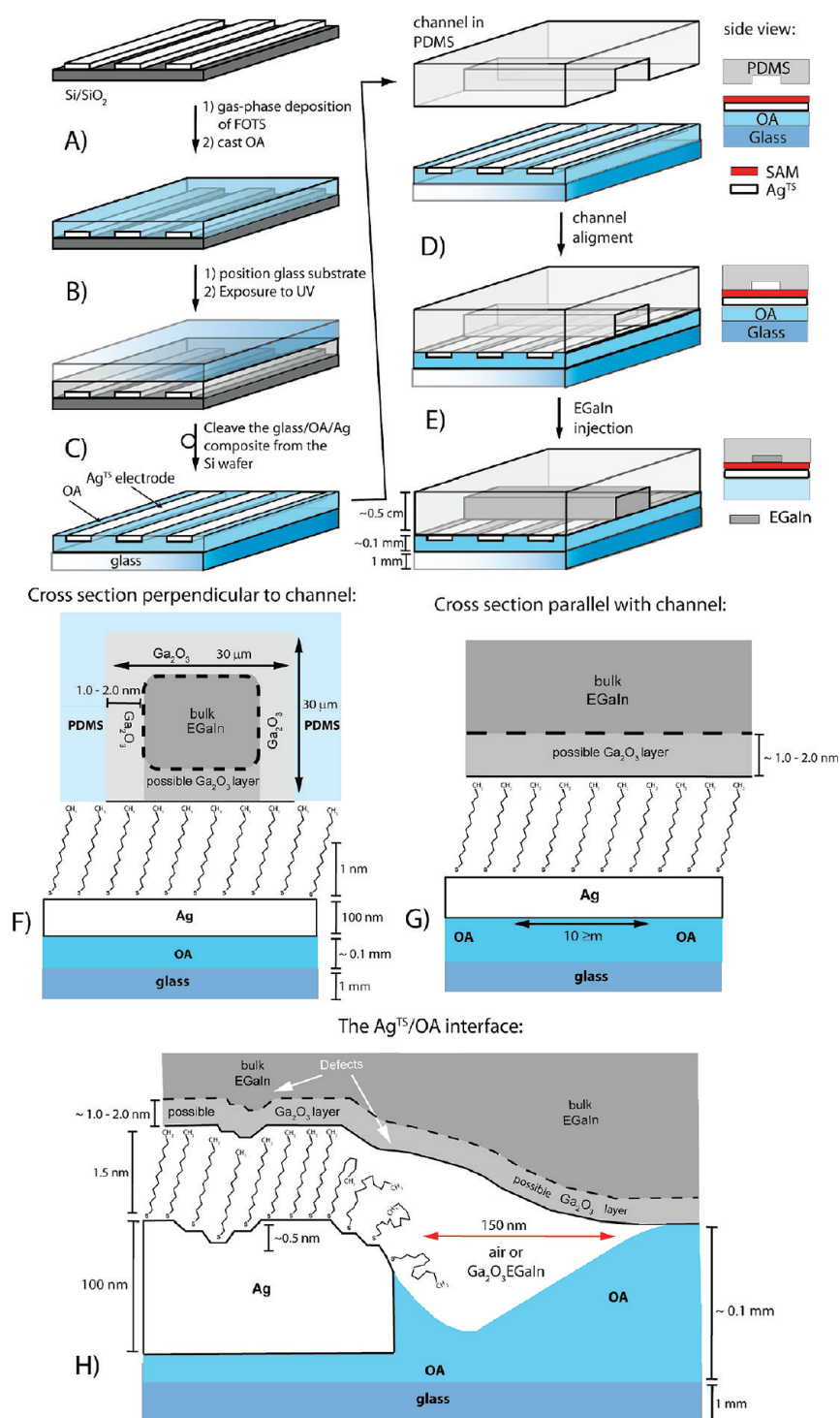


**FIGURE 1.** Fabrication of the arrays of SAM-based tunneling junctions. The schematic representations are not drawn to scale. (A) We fabricated the pattern of Ag electrodes using photolithography, electron-beam deposition of silver, and lift-off. (B) Using a UV-curable adhesive, we affixed a glass substrate to the pattern of the silver electrodes. The cured optical adhesive interacts strongly with the Ag and the glass support but not with the wafer. (C) We cleaved the Ag/adhesive/glass composite from the wafer by applying a razor blade—with gentle pressure in a direction parallel to the wafer—between the glass substrate and the wafer. (D) We aligned a microchannel in PDMS perpendicular to the electrodes after we formed the SAMs on these electrodes. (E) We filled the microchannels with Ga<sub>2</sub>O<sub>3</sub>/EGaIn to complete the device. (F) and (G) show schematic, idealized representations of the two side views of the junctions with a SAM of SC<sub>11</sub>CH<sub>3</sub>. (H) A schematic representation of the Ag<sup>TS</sup>/OA interface. The gap between the OA and the Ag<sup>TS</sup> (indicated by the red arrow), probably caused by shrinkage of the polymer during polymerization, is 150 nm wide and 6 nm deep. The SAMs will be disordered at the edge of the electrode; this disordered region has the potential to be a source of defects in the junctions. We believe that the surface tension of Ga<sub>2</sub>O<sub>3</sub>/EGaIn (surface tension of Ga<sub>2</sub>O<sub>3</sub>/EGaIn is 624 mN/m; see text) prevents it from filling the gap (filled with air) between the AO and the Ag<sup>TS</sup>, but we have no direct evidence to support this belief.

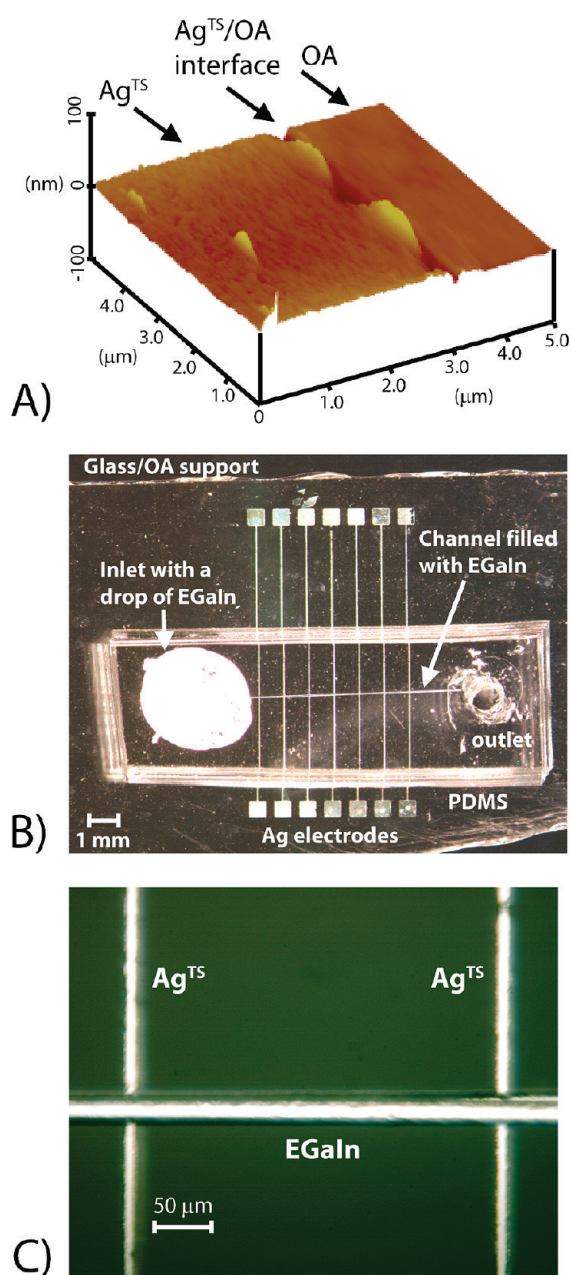


FIGURE 2. Atomic force micrograph (A) of the Ag<sup>TS</sup>/AO interface. Optical micrographs of a complete device (B) and a magnification of two junctions (C).

Figure 2 shows an atomic force micrograph of these Ag<sup>TS</sup> electrodes embedded in OA. The atomic force micrograph shows two important characteristics of the electrodes. (i) The difference in height between the OA and Ag electrodes was insignificant ( $<0.1$  nm). (ii) The Ag<sup>TS</sup> electrodes were smooth and had a root-mean-square surface roughness of 0.9 nm (approximately two lattice planes of silver) measured over  $25 \times 25 \mu\text{m}^2$ , but the Ag<sup>TS</sup>/OA interface did not seal completely with the OA at their edges: the gap at the Ag<sup>TS</sup>/OA interface was 150 nm wide and 6.0 nm deep, with a surface roughness of 5.8 nm (averaged over  $5.0 \times 0.1 \mu\text{m}^2$ ). This procedure, thus, generates embedded electrodes that

are flat, but the topography at the interface between the metal and OA is not completely smooth. Figure 1H sketches this AO/Ag<sup>TS</sup> interface schematically and shows that our junctions are not free of defects.

To account for defects in the tunneling junctions, to discriminate artifacts from real data, and to determine the yields of working devices, we believe it is essential to collect and to analyze statistically large numbers of data.<sup>11</sup> Although statistical analyses are common in (and an essential part of) studies involving break junctions,<sup>33</sup> junctions involving scanning probes,<sup>13</sup> and most other systems subjected to careful physical measurement, Lee et al.<sup>11</sup> was the first to address, with statistical analysis of many data, the shortcomings of SAM-based junctions having evaporated metal top-electrodes prepared using the very low yielding (1–2%) procedures generated in most prior work.

We used a procedure for the statistical analysis of the data ( $N = 300\text{--}800$  obtained from two to five devices for each type of SAM, Table S1 in Supporting Information) that we have described previously (see Supporting Information).<sup>29</sup> We constructed histograms of *all* values of  $J$  for each measured potential. We fitted *all* our data to single Gaussian functions using a nonlinear least-squares fitting procedure to obtain the log-mean value of  $J$  for each measured potential and its log-standard deviation. We emphasize that no data are omitted: we have *not* selected data.

Panels A and B of Figure 3 show that the current density through the junctions of Ag<sup>TS</sup>–SC<sub>*n*</sub>–1CH<sub>3</sub>/EGaIn (with  $n = 12, 14, 16,$  or  $18$ ) (i) depends exponentially on the thickness ( $d$  (Å)) of the SAM, (ii) depends linearly on the bias in the low-bias regime, and (iii) is independent of the temperature  $T$ . All these observations indicate, as expected from a large body of previous work,<sup>6,11,34–36</sup> that the mechanism of charge transport is tunneling. The tunneling decay coefficient  $\beta$  (Å<sup>-1</sup>) can be determined using eq 2 ( $J_0$  (A/cm<sup>2</sup>) is a constant that depends on the system and includes contact resistance).

$$J = J_0 e^{-\beta d} \quad (2)$$

We found that  $\beta = 0.80 \pm 0.2 \text{ \AA}^{-1}$  (or  $\beta = 1.0 \pm 0.2$  per CH<sub>2</sub>) with  $J_0 = 6.3 \times 10^2 \text{ A/cm}^2$  at a bias of  $-0.5 \text{ V}$  and  $\beta = 0.74 \pm 0.2 \text{ \AA}^{-1}$  (or  $\beta = 0.93 \pm 0.2$  per CH<sub>2</sub>) with  $J_0 = 21 \text{ A/cm}^2$  at  $-0.2 \text{ V}$ ;<sup>37</sup> both values of  $\beta$  are within the range reported for similar compounds,<sup>4</sup> including those obtained with cone-shaped tips of Ga<sub>2</sub>O<sub>3</sub>/EGaIn.<sup>28</sup> (Our initial description<sup>28</sup> of these cone-shaped electrodes gave values of  $J$  that we interpreted to indicate a significantly lower value:  $\beta = 0.6$  per CH<sub>2</sub>. We now believe this interpretation was incorrect and that a value of  $\beta = 1.0$  per CH<sub>2</sub> is correct. We will discuss the origin of this error in a separate paper<sup>38</sup>).

Figure 3A shows temperature-dependent measurements of  $J$ – $V$  of a Ag<sup>TS</sup>–SC<sub>15</sub>CH<sub>3</sub>/Ga<sub>2</sub>O<sub>3</sub>/EGaIn junction (see Supporting Information). The devices we used in this study could

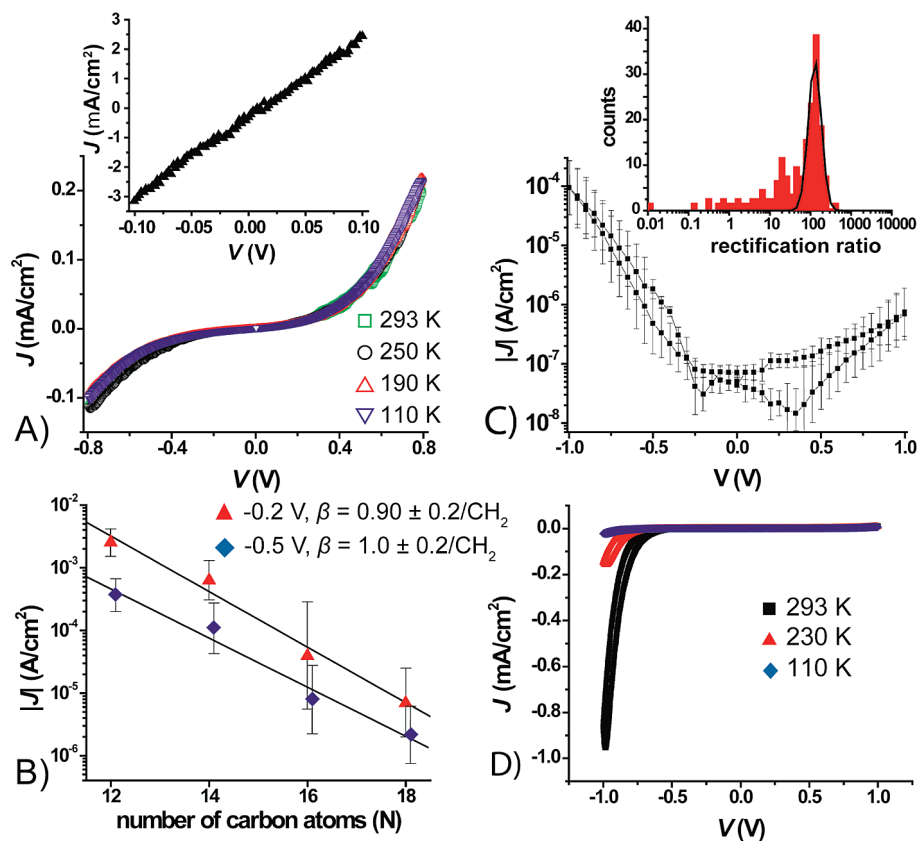


FIGURE 3. Current density measurements of  $\text{Ag}^{\text{TS}}\text{-SC}_{n-1}\text{CH}_3/\text{EGaIn}$  (with  $n = 12, 14, 16,$  or  $18$ ) and  $\text{Ag}^{\text{TS}}\text{-SC}_{11}\text{Fc//Ga}_2\text{O}_3/\text{EGaIn}$  junctions. (A) Four  $J$ - $V$  curves of a  $\text{Ag}^{\text{TS}}\text{-SC}_{13}\text{CH}_3/\text{Ga}_2\text{O}_3/\text{EGaIn}$  junction measured at four different temperatures ( $T = 110, 190, 250,$  and  $293$  K) in vacuum ( $1 \times 10^{-6}$  bar). Inset, the current density vs the voltage in the low-bias regime ( $-0.10$  to  $0.10$  V). (B) The values of  $J$  measured at  $-0.5$  and  $-0.2$  V as a function of the length of the SAM. The black, solid lines are fits to eq 2. (C) A semilog plot of the average absolute value of the current density vs the voltage of  $\text{Ag}^{\text{TS}}\text{-SC}_{11}\text{Fc//Ga}_2\text{O}_3/\text{EGaIn}$  junctions. The error bars indicate the log-standard deviation ( $N = 238$ ). At low voltages we observed a nonzero current (see Supporting Information). The current could involve oxidation-reduction processes of the Fc moieties. We did not observe (or perhaps too small to be observed) those currents in junctions with SAMs of  $\text{SC}_{n-1}\text{CH}_3$ . Inset, the histogram of the rectification ratios with a Gaussian fit to this histogram. We did not select data prior to analysis, and the Gaussian function is a fit to all data (see Supporting Information for details). (D) Three  $J$ - $V$  curves measured at three different temperatures ( $T = 110, 250,$  and  $293$  K).

be cooled from 293 to 110 K and warmed again to 293 K, without changing their  $J$ - $V$  characteristics (in vacuum at  $1 \times 10^{-6}$  bar). From this experiment we conclude that neither (i) solidification of EGaIn at  $\sim 250$  K nor (ii) the differences between the thermal expansion coefficients for PDMS ( $3 \times 10^{-4} \text{ K}^{-1}$ ),<sup>39</sup> glass ( $0.08 \times 10^{-4} \text{ K}^{-1}$ ),<sup>40</sup>  $\text{Ga}_2\text{O}_3$  ( $0.042 \times 10^{-4} \text{ K}^{-1}$ ),<sup>41</sup> Ag ( $0.18 \times 10^{-4} \text{ K}^{-1}$ ),<sup>42</sup> and EGaIn ( $1.1 \times 10^{-4} \text{ K}^{-1}$ )<sup>43</sup> cause shorts, lead to loss of contact, or alter the device characteristics in destructive ways (perhaps because the contact of the top-electrode with the SAM is determined by the layer of  $\text{Ga}_2\text{O}_3$ ).

The junctions have three uncertainties all related to the layer of  $\text{Ga}_2\text{O}_3$ . (i) *The resistance of the layer of  $\text{Ga}_2\text{O}_3$* : we estimated the resistance of the layer of  $\text{Ga}_2\text{O}_3$  and concluded that the resistance is approximately 4 orders of magnitude less than that of a SAM of  $\text{SC}_{10}\text{CH}_3$  (see Supporting Information).<sup>29</sup> (ii) *The thickness of the layer of  $\text{Ga}_2\text{O}_3$* : we measured the thickness of the layer of  $\text{Ga}_2\text{O}_3$  on a drop of  $\text{Ga}_2\text{O}_3/\text{EGaIn}$  to be less than 2.0 nm (see Supporting Information).<sup>30</sup> (iii) *The topography of contact of  $\text{Ga}_2\text{O}_3/\text{EGaIn}$  with the SAM*: we

recorded optical micrographs of the  $\text{Ga}_2\text{O}_3/\text{EGaIn}$  in microchannels in PDMS sealed against glass surfaces which suggest that the  $\text{Ga}_2\text{O}_3/\text{EGaIn}$  forms a conformal contact with the glass surface. We believe that a layer of  $\text{Ga}_2\text{O}_3$  at the PDMS interface forms during filling of the channels, since PDMS is permeable to oxygen.<sup>30</sup> This layer interacts strongly with the walls of the microchannel and is important for stabilizing the EGaIn in the microchannel (EGaIn has a higher surface tension<sup>44</sup> than Hg, but Hg—because its surface tension is not lowered by formation of an oxide layer—does not form stable features in microchannels in PDMS).<sup>30</sup> We have no direct evidence describing the interface between the  $\text{Ga}_2\text{O}_3/\text{EGaIn}$  and the SAM, but we infer that a discontinuous layer of  $\text{Ga}_2\text{O}_3$  forms at this interface (see Supporting Information). In our discussions we assume that the layer of  $\text{Ga}_2\text{O}_3$  is present. In any case, we believe that this layer of  $\text{Ga}_2\text{O}_3$  has only a very small influence on the values of  $J$  because of the low resistance of this layer and the (nearly) symmetrical  $J$ - $V$  curves obtained for the junctions with SAMs of  $n$ -alkanethiolates.

Figure 3C shows the average current density as a function of voltage for the  $\text{Ag}^{\text{TS}}\text{-SC}_{11}\text{Fc}/\text{Ga}_2\text{O}_3/\text{EGaIn}$  junctions, and the histogram of the rectification ratios with a Gaussian fit to this histogram. (See Supporting Information for the fitting procedure.) The data that lie outside the Gaussian come from one junction (20 counts), which was unstable, and a small population of noisy data arising from the set of otherwise functional junctions. These junctions show large rectification ratios (eq 1,  $R \approx 1.3 \times 10^2$  with a log-standard deviation of 1.4). Thus, 68% of the log-normal distribution of  $R$  lies within the interval (90, 180).

The junctions have three sources of asymmetry that may contribute to the rectification. (i) The two contacts between the electrodes and the SAMs differ: the  $\text{Ga}_2\text{O}_3/\text{EGaIn}$  top-electrode forms a van der Waals contact, and the silver bottom-electrode forms a covalent  $\text{Ag-S-CH}_2$  contact. (ii) The top- ( $\text{Ga}_2\text{O}_3/\text{EGaIn}$ ) and bottom-electrodes (Ag) may have different work functions ( $\Phi_{\text{Ag}} \approx \Phi_{\text{EGaIn}} \approx 4.5$  eV, but the work functions of each surface may be modified by the SAM or  $\text{Ga}_2\text{O}_3$ , respectively). (iii) A layer of  $\text{Ga}_2\text{O}_3$  is present only on the top-electrode and not on the bottom-electrode.

We believe that the rectification in the  $\text{Ag}^{\text{TS}}\text{-SC}_{11}\text{Fc}/\text{Ga}_2\text{O}_3/\text{EGaIn}$  junctions is due to the molecules and not to any other asymmetries in our junctions, or redox reactions involving Fc and  $\text{GaO}_x$ ,<sup>29</sup> for two reasons: (i) junctions lacking the Fc moiety, e.g., with SAMs of  $\text{SC}_{n-1}\text{CH}_3$ , do not rectify; thus, neither the layer of  $\text{Ga}_2\text{O}_3$  itself nor any other asymmetries in the junctions cause rectification. (ii) Two types of junctions with SAMs of  $\text{SC}_{11}\text{Fc}$  having top-electrodes other than  $\text{Ga}_2\text{O}_3/\text{EGaIn}$ , namely, a tungsten STM tip<sup>45</sup> or a redox-inactive Au foil,<sup>29</sup> also rectified currents with values of  $R \sim 10\text{--}100$ .

To clarify the mechanisms of charge transport across the  $\text{Ag}^{\text{TS}}\text{-SC}_{11}\text{Fc}/\text{Ga}_2\text{O}_3/\text{EGaIn}$  junctions, we measured the dependence of  $J\text{-}V$  on temperature. Figure 3D shows three  $J\text{-}V$  curves measured at 110, 230, and 293 K and Figure 4A shows both the values of  $J$  at +1.0 and  $-1.0$  V for the  $\text{Ag}^{\text{TS}}\text{-SC}_{11}\text{Fc}/\text{Ga}_2\text{O}_3/\text{EGaIn}$  junctions measured at  $T = 110\text{--}293$  K with intervals of 20 K. The values of  $J$  depend on  $T$  at negative bias but are (nearly<sup>46</sup>) independent of  $T$  at positive bias. This observation indicates that tunneling (which is temperature independent) is the dominant mechanism of charge transport at positive bias, while hopping (see below) is the dominant mechanism of charge transport at negative bias. This observation also illustrates the value of examination of rectification: whatever the uncertainties about a junction, its behavior at one bias is a good control for its behavior at opposite bias. Here, the comparison of forward and reverse bias at different temperatures supports the conclusion that cooling the devices does not introduce artifacts into our measurements.

Figure 4 shows the Arrhenius plots of a  $\text{Ag}^{\text{TS}}\text{-SC}_{11}\text{Fc}/\text{Ga}_2\text{O}_3/\text{EGaIn}$  junction at potentials in the range of  $-0.40$  to  $-1.0$  V and  $0.40$  to  $1.0$  V. This plot yields three important pieces of information. (i) Hopping is only observed between

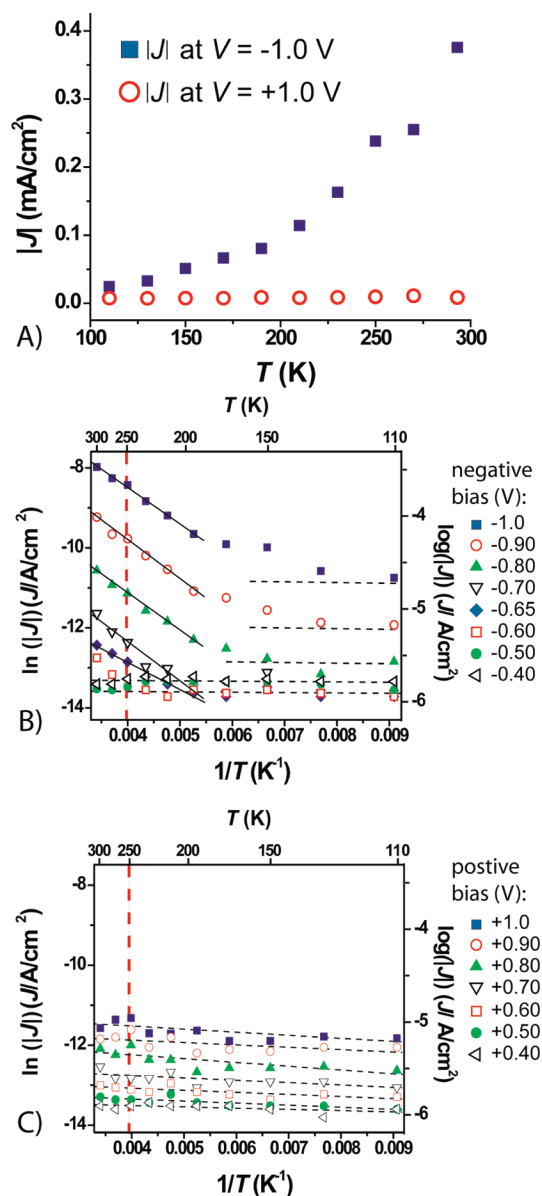
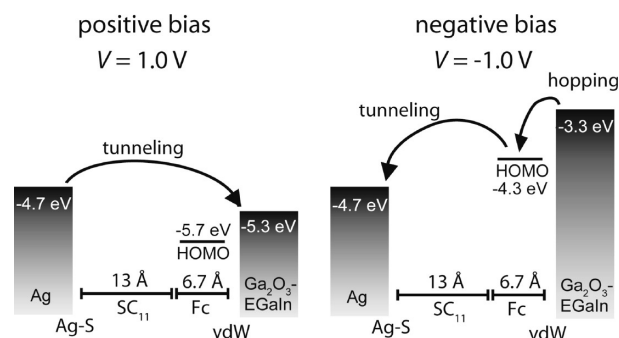


FIGURE 4. Thermally activated charge transport across  $\text{Ag}^{\text{TS}}\text{-SC}_{11}\text{Fc}/\text{Ga}_2\text{O}_3/\text{EGaIn}$  junctions. (A) The values of  $J$  measured at  $-1.0$  and  $1.0$  V as a function of temperature. Arrhenius plot of  $\text{Ag}^{\text{TS}}\text{-SC}_{11}\text{Fc}/\text{Ga}_2\text{O}_3/\text{EGaIn}$  junction for values of  $J$  measured at different potentials as a function of temperature in the range of  $-0.40$  to  $-1.0$  V (B) and  $0.40$  to  $1.0$  V (C). The red dashed vertical line indicates the temperature at which the EGaIn solidifies (as we could observe when we contacted the  $\text{Ga}_2\text{O}_3/\text{EGaIn}$  electrode with the probe). The solid black lines are fits to eq 3 and indicate regimes where the mechanism of charge transport is dominated by hopping. The dashed black lines are guides to the eyes to indicate regimes where the mechanism of charge transport is dominated by tunneling.

$-0.60$  and  $-1.0$  V, while at all other measured potentials the dominant mechanism of charge transport is tunneling; this observation suggests that, at  $-0.60$  V, the HOMO of the Fc begins to contribute to charge transport. (ii) The activation energy, determined from the slope of the Arrhenius plot using eq 3 (where the Boltzmann constant  $k_B = 8.62 \times 10^{-5}$  eV  $\text{K}^{-1}$ ) is  $E_a = 77 \pm 5.3$  meV ( $7.4 \pm 0.51$  kJ/mol) and is independent of the temperature. (iii) At temperatures below



**FIGURE 5.** Energy level diagram and mechanism of charge transport across  $\text{Ag}^{\text{TS}}\text{-SC}_{11}\text{Fc}/\text{Ga}_2\text{O}_3/\text{EGaIn}$  junctions. The barrier widths of the junctions are defined by the lengths of the  $\text{C}_{11}$  alkyl chains and the Fc moiety. At positive bias, the arrows suggest that the charge traversing the junctions has to tunnel across the whole length of the molecule ( $\text{C}_{11}$  alkyl chain and Fc group; a distance of 2 nm), because the HOMO level of the Fc moiety does not overlap with the Fermi levels of the electrodes. At negative bias, the HOMO level of the Fc moiety can participate in charge transport, and the charge only has to tunnel across the  $\text{C}_{11}$  moiety over a distance of 1.3 nm. In a second step, the charge can hop across the Fc moiety. We estimated the value of the HOMO level of the Fc moiety with wet electrochemistry (see Supporting Information).

190 K,  $k_{\text{B}}T \leq 16$  meV and is much smaller than  $E_{\text{a}}$  ( $77 \pm 5.3$  meV). Hence, at  $T < 190$  K, tunneling is the dominant mechanism of charge transport over the entire range of applied bias ( $-1.0$  to  $1.0$  V).

$$J = J_0 \exp(-E_{\text{a}}/k_{\text{B}}T) \quad (3)$$

All these observations can be rationalized by the model of charge transport proposed in Figure 5.<sup>47</sup> This figure shows proposed energy-level diagrams of the  $\text{Ag}^{\text{TS}}\text{-SC}_{11}\text{Fc}/\text{Ga}_2\text{O}_3/\text{EGaIn}$  junctions at biases of  $-1.0$  and  $1.0$  V. In all experiments, we biased the  $\text{Ga}_2\text{O}_3/\text{EGaIn}$  top-electrodes and grounded the  $\text{Ag}^{\text{TS}}$  bottom-electrode. The HOMO level of the  $\text{SC}_{11}\text{Fc}$  ( $-5.0$  eV; determined by wet electrochemistry; see Supporting Information) is centered on the Fc moiety and couples more strongly to the  $\text{Ga}_2\text{O}_3/\text{EGaIn}$  top-electrode (Fermi level of  $\sim -4.3$  eV) than to the  $\text{Ag}^{\text{TS}}$  bottom-electrode (Fermi level of  $\sim -4.7$  eV), because it is in van der Waals contact with the  $\text{Ga}_2\text{O}_3/\text{EGaIn}$  electrode, but it is separated from the  $\text{Ag}^{\text{TS}}$  electrode by the  $\text{SC}_{11}$  group. At positive bias, the Fermi level of the  $\text{Ga}_2\text{O}_3/\text{EGaIn}$  top-electrode decreases to below the value of the Fermi level of the  $\text{Ag}^{\text{TS}}$  electrode. The HOMO of the Fc follows the Fermi level of the top-electrode (we assumed a potential drop of 0.3 eV across the van der Waals interface<sup>47</sup>), and therefore does not fall between the Fermi levels of the two electrodes. It does not participate in charge transport, but instead it becomes part of the tunneling barrier. At negative bias, the Fermi level of the top-electrode increases, as does the HOMO of the Fc. At sufficiently negative bias, the HOMO of the Fc can overlap with both Fermi levels of the electrodes and contribute to charge transport. We do not know all the details of the

mechanism of charge transport, but we speculate that, when the HOMO level of the Fc is energetically accessible, the first step involves an electron from the HOMO level of the Fc tunneling across the  $\text{SC}_{11}$  moiety (resulting in an  $\text{Fc}^+$  ion), and the second step involves an electron hopping from the top-electrode to the Fc moiety, as suggested by the arrows (the arrows would point in the opposite direction in the case of hole transport). Arrhenius type of hopping implies that conformational changes—perhaps a Marcus type of charge transfer involving movement of the  $\text{Fc}^+$  moiety with respect to the top-electrode—are important to facilitate the transfer of charges from the top-electrode to the  $\text{Fc}^+$  moiety. Activation of the hopping mechanism at negative bias led to values of  $J$  that were 2 orders of magnitude higher (at room temperature) than those observed with tunneling alone at positive bias; thus, in our junctions, hopping is more efficient in the transport of charge than tunneling (Figure 4). We infer that tunneling is the rate-limiting step in the transport of charge and that the lifetime of the  $\text{Fc}^+$  species is probably short. We do not know how many Fc groups are oxidized at any given time or how the  $\text{Fc}^+$  ions interact with the  $\text{Ga}_2\text{O}_3$  layer. The  $\text{Fc}^+$  ions will probably have a stronger interaction (perhaps ionic) with the  $\text{Ga}_2\text{O}_3$  layer than neutral Fc moieties. We believe that the layer of  $\text{Ga}_2\text{O}_3$  does not significantly affect the mechanism of charge transport across the SAMs (see above and Supporting Information).

The large observed rectification ratio ( $R \approx 130$ ) for the  $\text{Ag}^{\text{TS}}\text{-SC}_{11}\text{Fc}/\text{Ga}_2\text{O}_3/\text{EGaIn}$  junctions cannot be explained solely either by the presence of an asymmetrical tunneling barrier within the junction or by citing the difference in potential drops across the Fc moiety and the alkyl chain. Theoretical studies incorporating either of these effects have suggested that for molecular tunneling junctions the rectification ratios cannot exceed  $\sim 20$ .<sup>48</sup> Those studies did not, however, consider a change in the mechanism of charge transport between forward and reverse bias as a mechanism for rectification that might result in high rectification ratios.

The values of  $R$  can be rationalized by the fact that hopping (when  $k_{\text{B}}T \geq E_{\text{a}}$ ) is more efficient in the transport of charge (i.e., allows for a higher current) than tunneling (Figure 4). When the HOMO of the Fc does not participate in charge transport, the charge must tunnel (elastically or inelastically) through the entire width of the junction, i.e., roughly the whole length of  $\text{SC}_{11}\text{Fc}$  molecule defined by the lengths of the  $\text{SC}_{11}$  chain ( $d_{\text{SC}_{11}}$ , 1.3 nm) and the Fc moiety ( $d_{\text{Fc}}$ , 0.66 nm). When the HOMO of the Fc falls between the Fermi levels of the electrodes, charge can tunnel from the HOMO of the Fc across the  $\text{C}_{11}$  chain, followed by hopping of charge to the Fc moiety. This change in the mechanism of charge transport from tunneling to hopping effectively reduces the width of the tunneling barrier from  $d_{\text{SC}_{11}} + d_{\text{Fc}}$  to  $d_{\text{SC}_{11}}$ . Thus, the rectification ratio is approximately the ratio of the tunneling current densities across the whole SAM ( $j_{\text{SC}_{11}\text{Fc}}$ ) to the tunneling current density across the  $\text{SC}_{11}$  moiety ( $j_{\text{SC}_{11}}$ ) and can be estimated using eq 4 (with  $\beta_{\text{SC}_{11}} =$

the decay constant across  $SC_{11}$  ( $\text{\AA}^{-1}$ , or per  $\text{CH}_2$ ) and  $\beta_{\text{Fc}}$  = the decay constant across the Fc moiety ( $\text{\AA}^{-1}$ , or per  $\text{CH}_2$ )).

$$R = J_{SC_{11}}/J_{SC_{11}Fc} \propto \exp(-\beta_{SC_{11}}d_{SC_{11}})/(\exp(-\beta_{SC_{11}}d_{SC_{11}}) \exp(-\beta_{\text{Fc}}d_{\text{Fc}})) \quad (4)$$

We do not know the value of  $\beta_{\text{Fc}}$  but have assumed  $\beta_{\text{alkyl}} = \beta_{\text{Fc}} = 0.80 \text{\AA}^{-1}$  (or 1.0 per  $\text{CH}_2$ ) to obtain a lower-limit value of  $J_{SC_{11}}/J_{SC_{11}Fc} = 2.0 \times 10^2$ . This semiquantitative theoretical estimation of  $R$  is compatible with the observed rectification ratio of  $R \approx 1.3 \times 10^2$ . This proposed model also agrees with the observation that the rectification ratios are close to unity at temperatures less than 190 K (Figure 4A), because hopping becomes less efficient than tunneling when  $k_{\text{B}}T \ll E_{\text{a}}$ . At low temperatures, therefore, the hopping mechanism is eliminated and the Fc moiety becomes part of the tunneling barrier in both directions of bias.

To realize potential applications of SAM-based devices, the mechanisms of charge transport across these SAM-based junctions must be understood. This paper describes a method of fabricating arrays of seven SAM-based junctions per device that relies on the stabilization of liquid-metal electrodes in microchannels. This method achieves high post-fabrication yields (70–90%) and junctions that are stable up to hundreds of cycles. Furthermore, this technique enables the measurement of  $J$ – $V$  characteristics as a function of the chemical structure of the SAM, with statistically large numbers of data, and as a function of temperature over the range of 110–293 K. We believe that such studies are required to confirm that the characteristics of molecular devices are indeed dominated by the chemical composition of the SAMs, to discriminate artifact from real data, and to establish the mechanism of charge transport across SAMs.

We characterized two types of SAM-based junctions incorporating SAMs of  $SC_{n-1}\text{CH}_3$  ( $n = 12, 14, 16,$  and  $18$ ) and  $SC_{11}\text{Fc}$ . Junctions incorporating SAMs of  $SC_{11}\text{Fc}$  have large rectification ratios of  $R \approx 1.3 \times 10^2$ , while those with SAMs of  $SC_{n-1}\text{CH}_3$  do not rectify ( $R \approx 1$ – $5$ ). Our physical–organic study with statistically large numbers of data ( $N = 300$ – $800$ ) shows that the rectification is due to the chemical structure of the SAM and not caused by any of the other asymmetries of the junctions. Although molecular rectifiers have been reported before,<sup>19–22,24,26</sup> no measurements of  $J$ – $V$  as a function of temperature have been conducted, and the absence of such measurements has left the mechanism of charge transport unclear. Here, measurements of  $J$ – $V$  as a function of temperature clearly suggest a mechanism of charge transport across the  $\text{Ag}^{\text{TS}}\text{--}SC_{11}\text{Fc}/\text{Ga}_2\text{O}_3/\text{EGaIn}$  junctions (Figure 5) consisting of tunneling supplemented by hopping at temperatures above 190 K and biases from  $-0.6$  to  $-1.0$  V. The charge can hop from the top-electrode to the Fc moiety when the HOMO of the Fc overlaps with the Fermi levels of the electrodes and thus reduces the width of the tunneling

barrier, an event which occurs at negative bias but not at positive bias. Thus, a difference in the mechanism of charge transport at opposite biases across the *same* junction is the basis of the large molecular rectification ( $R \approx 1.3 \times 10^2$ ) we observe in this system and is potentially useful for constructing other molecular- or SAM-based, two-terminal devices with well-defined electronic functions.

**Acknowledgment.** The Netherlands Organization for Scientific Research (NWO) is kindly acknowledged for the Rubicon grant, which supports the research of C.A.N. Professor Hongkun Park is gratefully acknowledged for allowing us to conduct the temperature-dependent  $J$ – $V$  measurements in his laboratory. We acknowledge NSF (Grant CHE-05180055) for funding.

**Supporting Information Available.** The experimental procedures, details of the electrical properties of the layer of  $\text{Ga}_2\text{O}_3$ , microchannels on glass filled with  $\text{Ga}_2\text{O}_3/\text{EGaIn}$ , wet electrochemistry, and data collection and statistical analysis. This material is available free of charge via the Internet at <http://pubs.acs.org>.

## REFERENCES AND NOTES

- (1) A molecular device is truly molecular if it has at least one of the dimensions of a thickness of one molecule. Single molecule junctions are junctions that ideally contain only one molecule. Junctions based on self-assembled monolayers (SAMs) contain a large number of molecules ( $10^3$  to  $10^{12}$  depending on the size of the junctions) in the  $xy$  plane but are only one molecule thick in the  $z$  direction.
- (2) Collier, C. P.; Wong, E. W.; Belohradsky, M.; Raymo, F. M.; Stoddart, J. F.; Kuekes, P. J.; Williams, R. S.; Heath, J. R. *Science* **1999**, *285*, 391.
- (3) Green, J. E.; Choi, J. W.; Boukai, A.; Bunimovich, Y.; Johnston-Halperin, E.; Delonno, E.; Luo, Y.; Sheriff, B. A.; Xu, K.; Shin, Y. S.; Tseng, H. R.; Stoddart, J. F.; Heath, J. R. *Nature* **2007**, *445*, 414.
- (4) Reed, M. A.; Chen, J.; Rawlett, A. M.; Price, D. W.; Tour, J. M. *Appl. Phys. Lett.* **2001**, *78*, 3735.
- (5) Bang, G. S.; Chang, H.; Koo, J.-R.; Lee, T.; Advincula, R. C.; Lee, H. *Small* **2008**, *4*, 1399.
- (6) Akkerman, H. B.; de Boer, B. J. *Phys.: Condens. Matter* **2008**, *20*, No. 013001.
- (7) Fisher, G. L.; Walker, A. V.; Hooper, A. E.; Tighe, T. B.; Bahnck, K. B.; Skriba, H. T.; Reinard, M. D.; Haynie, B. C.; Opila, R. L.; Winograd, N.; Allara, D. L. *J. Am. Chem. Soc.* **2002**, *124*, 5528.
- (8) Walker, A. V.; Tighe, T. B.; Cabarcos, O. M.; Reinard, M. D.; Haynie, B. C.; Uppili, S.; Winograd, N.; Allara, D. L. *J. Am. Chem. Soc.* **2004**, *126*, 3954.
- (9) Beebe, J. M.; Kushmerick, J. G. *Appl. Phys. Lett.* **2007**, *90*, No. 083117.
- (10) Lau, C. N.; Stewart, D. R.; Williams, R. S.; Bockrath, M. *Nano Lett.* **2004**, *4*, 569.
- (11) Kim, T.-W.; Wang, G.; Lee, H.; Lee, T. *Nanotechnology* **2007**, *18*, 315204.
- (12) Selzer, Y.; Cabassi, M. A.; Mayer, T. S.; Allara, D. L. *J. Am. Chem. Soc.* **2004**, *126*, 4052.
- (13) Li, X. L.; Hihath, J.; Chen, F.; Masuda, T.; Zang, L.; Tao, N. J. *J. Am. Chem. Soc.* **2007**, *129*, 11535.
- (14) These junctions, which incorporate molecules covalently bound to Si by hydrosilylation of alkenes with Si:H, should not be confused with junctions incorporating alkyl silanes bound to thin films of  $\text{SiO}_x$  on Si. Junctions of the latter class show essentially no dependence of current density on molecular length and, thus, are of limited use for investigating charge transport. For example, see: Selzer, Y.; Salomon, A.; Cahen, D. J. *J. Am. Chem. Soc.* **2002**, *124*, 2886.

- (15) Salomon, A.; Boecking, T.; Chan, C. K.; Amy, F.; Girshevitz, O.; Cahen, D.; Kahn, A. *Phys. Rev. Lett.* **2005**, *95*, 266807.
- (16) Salomon, A.; Boecking, T.; Seitz, O.; Markus, T.; Amy, F.; Chan, C.; Zhao, W.; Cahen, D.; Kahn, A. *Adv. Mater.* **2007**, *19*, 445.
- (17) Salomon, A.; Böcking, T.; Gooding, J. J.; Cahen, D. *Nano Lett.* **2006**, *6*, 2873.
- (18) Aviram, A.; Ratner, M. A. *Chem. Phys. Lett.* **1974**, *29*, 277.
- (19) Metzger, R. M. *Acc. Chem. Res.* **1999**, *32*, 950.
- (20) Lenfant, S.; Krzeminski, C.; Delerue, C.; Allan, G.; Vuillaume, D. *Nano Lett.* **2003**, *3*, 741.
- (21) Ashwell, G. J.; Urasinska, B.; Tyrrell, W. D. *Phys. Chem. Chem. Phys.* **2006**, *8*, 3314.
- (22) Chen, X.; Jeon, Y.-M.; Jang, J.-W.; Qin, L.; Huo, F.; Wei, W.; Mirkin, C. A. *J. Am. Chem. Soc.* **2008**, *130*, 8166.
- (23) Böhme, T.; Simpson, C. D.; Müllen, K.; Rabe, J. P. *Chem.—Eur. J.* **2007**, *13*, 7349.
- (24) Chabinyac, M. L.; Chen, X.; Holmlin, R. E.; Jacobs, H.; Skulason, H.; Frisbie, C. D.; Mujica, V.; Ratner, M. A.; Rampi, M. A.; Whitesides, G. M. *J. Am. Chem. Soc.* **2002**, *124*, 11730.
- (25) Love, J. C.; Estroff, L. A.; Kriebel, J. K.; Nuzzo, R. G.; Whitesides, G. M. *Chem. Rev.* **2005**, *105*, 1103.
- (26) Metzger, R. M. *Chem. Rev.* **2003**, *103*, 3803.
- (27) Selzer, Y.; Cabassi, M. A.; Mayer, T. S.; Allara, D. L. *Nanotechnology* **2004**, *15*, S483.
- (28) Chiechi, R. C.; Weiss, E. A.; Dickey, M. D.; Whitesides, G. M. *Angew. Chem., Int. Ed.* **2008**, *47*, 142.
- (29) Nijhuis, C. A.; Reus, W. F.; Whitesides, G. M. *J. Am. Chem. Soc.* **2009**, *131*, 17814.
- (30) Dickey, M. D.; Chiechi, R. C.; Larson, R. J.; Weiss, E. A.; Weitz, D. A.; Whitesides, G. M. *Adv. Funct. Mater.* **2008**, *18*, 1097.
- (31) Weiss, E. A.; Chiechi, R. C.; Kaufman, G. K.; Kriebel, J. K.; Li, Z.; Duati, M.; Rampi, M. A.; Whitesides, G. M. *J. Am. Chem. Soc.* **2007**, *129*, 4336.
- (32) Black, A. J.; Paul, K. E.; Aizenberg, J.; Whitesides, G. M. *J. Am. Chem. Soc.* **1999**, *121*, 8356.
- (33) Venkataraman, L.; Klare, J. E.; Nuckolls, C.; Hybertsen, M. S.; Steigerwald, M. L. *Nature* **2006**, *442*, 7105.
- (34) McCreery, R. L. *Chem. Mater.* **2004**, *16*, 4477.
- (35) Slowinski, K.; Fong, H. K. Y.; Majda, M. *J. Am. Chem. Soc.* **1999**, *121*, 7257.
- (36) Engelkes, V. B.; Beebe, J. M.; Frisbie, C. D. *J. Am. Chem. Soc.* **2004**, *126*, 14287.
- (37) The value of  $\beta$  depends on the bias and changes from 0.80 per CH<sub>2</sub> measured at 0.050 V to 1.0 per CH<sub>2</sub> measured at 0.50 V. We will address this issue in a separate paper.
- (38) Reus, W. F.; Nijhuis, C. A.; Barber, J.; Cademartiri, L.; Mwagoni, M.; Whitesides, G. M. Manuscript in preparation.
- (39) Lee, S.-Y.; Tung, H.-W.; Chen, W. -C.; Fang, W. *IEEE Photonics Technol. Lett.* **2006**, *18*, 2191.
- (40) Menke, Y.; Peltier-Baron, V.; Hampshire, S. *J. Non-Cryst. Solids* **2000**, *276*, 145.
- (41) Yamaga, M.; Villora, E. G.; Shimamura, K.; Ichinose, N.; Honda, M. *Phys. Rev. B* **2003**, *68*, 155207.
- (42) Lide, D. R. *Handbook of Chemistry and Physics*; CRC Press, Inc.: Boca Raton, FL, 1996.
- (43) Koster, J. N. *Cryst. Res. Technol.* **1999**, *34*, 1129.
- (44) Zrnic, D.; Swatik, D. S. *J. Less-Common Met.* **1969**, *18*, 67.
- (45) Müller-Meskamp, L.; Karthäuser, S.; Zandvliet, H. J. W.; Homberger, M.; Simon, U.; Waser, R. *Small* **2009**, *5*, 496.
- (46) We observed a small dependence of  $J$  on the temperature (with an activation energy of 3–5 meV obtained from a fit to eq 3) in the tunneling regime, which could involve conformational changes of the molecules or charge transport mediated by impurities.
- (47) We assumed a potential drop of 0.3 eV across the van der Waals interface and, thus, the HOMO level of the Fc changes from –5.0 to –5.7 eV under a bias of 1.0 V, or to –4.3 eV under a bias of –1.0 V. We will discuss the potential drop across the junctions in detail in a separate paper. Nijhuis, C. A.; Reus, W. R.; Whitesides, G. M. Manuscript in preparation.
- (48) Stadler, R.; Geskin, V.; Cornil, J. *J. Phys.: Condens. Matter.* **2008**, *20*, 374105.